

Comparison of Reflector Antenna Measurements and Simulations

M. Sierra Castañer
Grupo de Radiación. ETSI Telecomunicación, Universidad
Politécnica de Madrid (UPM)
Madrid, Spain
mscastaner@gr.ssr.upm.es

L.J. Foged, M.A. Saporetti,
Microwave Vision Italy (MVI)
Pomezia, Italy
(lars.foged, maria.saporetti)@microwavevision.com

E. Jørgensen
TICRA
Copenhagen K, Denmark
ej@ticra.com

T. Voigt
Altair (FEKO)
Böblingen, Germany
voigt@altair.de

D. Tallini
CST AG
Darmstadt, Germany
Davide.Tallini@cst.com

M. Orefice, G. Giordanengo, G. Dassano
Antenna and EMC Lab (LACE)
Politecnico di Torino, Torino, Italy
(mario.orefice, giorgio.giordanengo,
gianluca.dassano)@polito.it

M. Böttcher, A. Wien
IMST GmbH
Kamp-Lintfort, Germany
(boettcher, wien)@imst.de

J. M. Serna
Technological Development Center of Yebes (CDT)
Yebes, Guadalajara - Spain
jm.serna@oan.es

D. Pérez de Diego
Centro de Alta Tecnología y Homologación -CATECHOM-
Universidad de Alcalá, Spain
diego.perezd@uah.es

F. Calvano
ANSYS Italia Srl,
Viale Luca Gaurico, 9/11, 00143 Roma, Italy
flavio.calvano@ansys.com

I. INTRODUCTION

Abstract— In antenna measurement, well-established procedures are consolidated to determine the associated measurement uncertainty for a given antenna and measurements scenario [1-2]. Similar criteria for establishing uncertainties in numerical modeling of the same antenna are still to be established. In this paper, we investigate the achievable agreement between antenna measurement and simulation when external error sources are minimized. The test object, is a reflector fed by a wideband dual ridge horn (SR40-A and SH4000) manufactured by MVG. This highly stable reference antenna has been selected to minimize uncertainty related to finite manufacturing and material parameter accuracy. Two frequencies, 10.7GHz and 18GHz have been selected for detailed investigation. The antenna has been measured by several measurement facilities (spherical, cylindrical and planar near field ranges) across Europe in the frame of the EurAAP/WG5 “Facility Comparison Campaign” activity. The purpose of this intercomparison campaign is the comparison of the different antenna measurement facilities, throughout Europe, considering measurement procedures and uncertainty estimates. The antenna has been simulated using a full CAD model, in step compatible format and using different numerical methods from different software vendors [3-7].

The achievable agreement between antenna measurement and simulation has already been investigated in [8], using a reflector fed by a wideband dual ridge horn (SR40-A and SH4000) by MVG, which has been measured in two antenna measurements systems and simulated with four different numerical tools. The study carried here is a further analysis which involves an higher number of:

- measurements: seven measurements have been performed in six different measurement facilities across Europe (in the frame of the EurAAP/WG5 “Facility Comparison Campaign” activity),
- simulations: five simulations have been performed with tools from five software vendors.

The objective of the paper is to show the agreement between different measurement setups, between different software tools, and, more important, the agreement between simulation and measurements to check the limitation of the simulation tools.

II. TEST OBJECT

The SR40-A and SH4000 antenna is shown in Fig. 1. The SR40-A is an offset parabolic reflector, precision machined from a single block of aluminum. The circular interface with precision holes allows the user to center the antenna with very high accuracy. The alignment accuracy is determined to within $\pm 0.01^\circ$. The SH4000 wide band Dual Ridge Horn is a highly stable reference antenna precision fitted to the mounting bracket of the reflector.



Figure 1. Reflector SR 40-A fed by SH4000 Dual Ridge Horn: Antenna during measurement (left); CAD file for simulation (right).

III. SIMULATION CAMPAIGN

Simulations have been performed at 10.7GHz and 18GHz, considering the nominal dimensions of the feed and reflector and ignoring finite manufacturing and material parameter tolerances. The electrical conductivity of aluminum was assumed to be $3.56 \cdot 10^7$ S/m in the simulation of ohmic losses. The complete CAD file of the antenna was provided to each of the participants involved. Each participant was responsible for generating a suitable mesh and the numerical stability of their solution. The information collected from simulations is reported in Table I.

TABLE I. SIMULATION DATA

Peak Directivity	10.7, 18 GHz
Directivity patterns	Phi: from 0° to 135° (45° step) Theta: from -180° to 180° (1° and 0.1° step)
Return Loss	10.7, 18 GHz
Ohmic Losses	10.7, 18 GHz

Each field solver has used the simulation method considered the most efficient for reflector design. The list of numerical methods is shown in Table II, while Fig.2 to 6 show the currents, the fields and the mesh grid resulting from each numerical tool.

TABLE II. NUMERICAL METHODS USED FOR THE SIMULATIONS

SIMULATION TOOL	NUMERICAL METHOD
GRASP	Higher-order Multi-level Fast Multipole
ANSYS	Hybrid FEBI (enhancement to the FEM solver)
FEKO	Multi-level Fast Multipole
CST	Time Domain Solver (based on the Finite Integration Technique)
EMPIRE	Finite Difference Time Domain

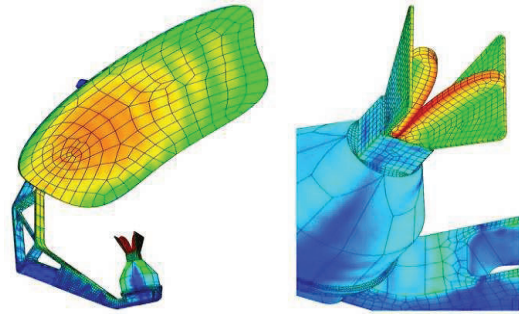


Figure 2. GRASP- currents induced on the antenna and mesh grid @18GHz. Reflector SR 40-and SH4000 fed (left), Close-up of the feed (right).

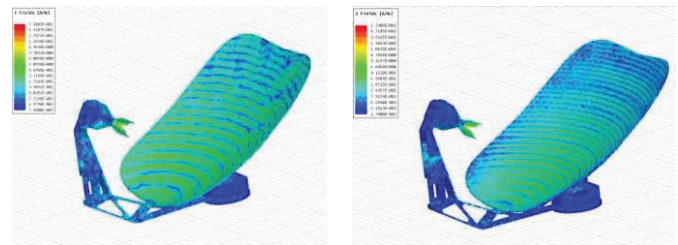


Figure 3. HFSS simulated surface current density J_s @10.7GHz (left) and 18GHz (right) Reflector SR 40-A with SH4000 Dual Ridge Horn.

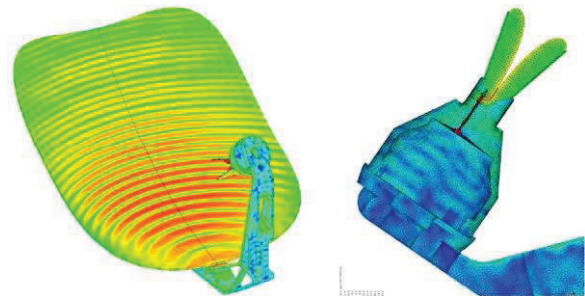


Figure 4. FEKO - currents induced on the antenna structure and applied mesh @18GHz on the Reflector SR 40-A with SH4000 Dual Ridge Horn. Currents (left); Close-up of the feed (right).

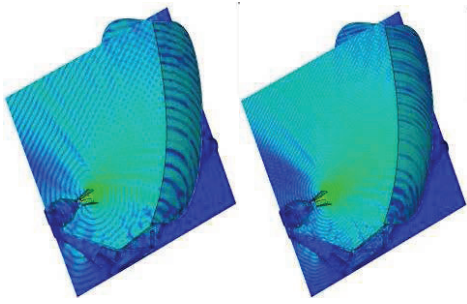


Figure 5. CST- Simulated E-field @10.7GHz (left) and @18GHz (right). Reflector SR 40-A with SH4000 Dual Ridge Horn.

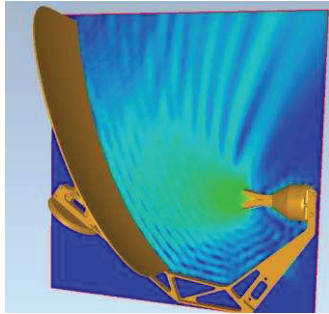


Figure 6. EMPIRE simulated Near Field@10.7GHz

IV. MEASUREMENT CAMPAIGN

The measurement uncertainty or error estimate for a given antenna, using a given measurement range, remains an approximation, until this estimate has been successfully validated against other measurements. Such validation can be achieved by means of facility intercomparison campaigns, which provides the formal opportunity for the participants to validate and document their achieved measurement accuracy and procedures from comparison with other facilities. Facility-comparison campaigns are an important on-going activity in the frame of the EurAPP working group on antennas measurements and the SR40-A and SH4000 antenna is part of a currently ongoing measurement facility comparison campaign.

The information collected from measurements is reported in Table III.

TABLE III. MEASUREMENT DATA

Peak Directivity	10.7, 12.6, 14.5, 18, 19, 20, 28, 29, 30, 31, 33, 38 GHz
Directivity patterns	Phi: from 0° to 135°(45° step) Theta: from -180° to 180° (1° steps)
Return Loss	10.7-38 GHz
Ohmic Losses	10.7-38 GHz
Uncertainty Budget	10.7-38 GHz

The list of the facilities, involved in the EurAAP intercomparison campaign and whose data have been used for the results reported below, is shown in Table IV while Fig.7 shows the geographical location.

TABLE IV. ANTENNA MEASUREMENT SYSTEMS

FACILITY	RANGE
Universidad Politécnica de Madrid (UPM) -2 measurements	Spherical Near Field
MVG SG64 (Paris)	Spherical Near Field
University of Alcalà	Spherical Near Field
Politecnico di Torino	Spherical Near Field
Astronomic Observatory of Yebes	Planar Near Field
IMST	Cylindrical Near Field

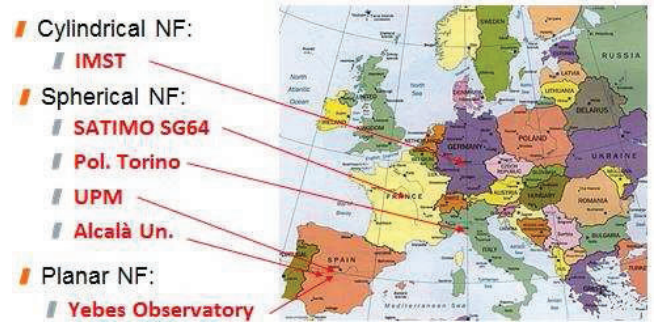


Figure 7. European location of some facilities involved in the Reflector SR40+SH4000 campaign.

V. RESULTS COMPARISON

A reference pattern has been computed both for simulations and for measurements.

The simulation reference pattern has been obtained as the simple mean of all the simulated radiation patterns, using amplitude data only.

The measurement reference patterns can be calculated as the simple mean or weighted mean of each measured data point where the weights are proportional to the estimated uncertainty. In [9], different data processing procedures have been investigated to derive reference patterns with increased confidence level based on measurements in different facilities. Anyway, research is still ongoing to define the best way of defining the reference pattern through a proper combination of measurements and weights. For this activity, the simple mean of the radiation patterns, using amplitude data only, has been used to define the measurement reference pattern.

In the following, comparisons including the peak directivity, patterns, equivalent error level and losses are reported.

A. Peak Directivity Comparison

The peak directivity values are reported for measurement and simulation references in Table V. The table confirms the very good agreement between measurements and simulations.

TABLE V. MEASURED AND SIMULATED PEAK DIRECTIVITY

Peak Directivity [dBi]		
Frequency	Measured	Simulated
10.7 GHz	31.15	31.10
18 GHz	35.50	35.60

B. Pattern Comparison

The Ludwig III [10] co-polar and cross-polar components [Ludwig III of the measurement and simulation reference patterns at 2 cuts, phi=0° and 90°, @ 10.7GHz and 18GHz are reported. The agreement can also be evaluated as a single value. The pattern correlation or equivalent noise level is reported in the following paragraph.

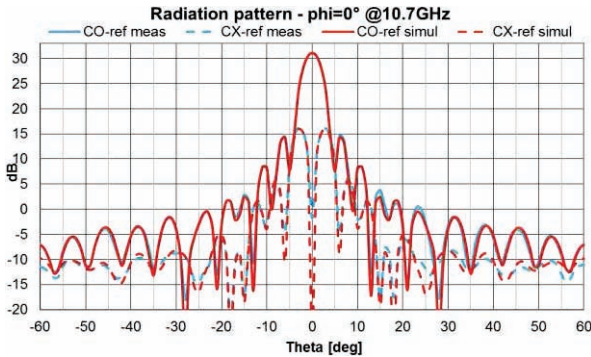


Figure 8. Measurement and simulation reference directivity patterns @10.7GHz, phi=0°.

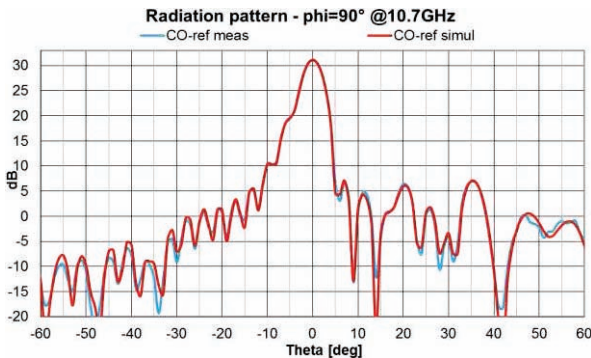


Figure 9. Measurement and simulation reference directivity patterns @10.7GHz, phi=90°.

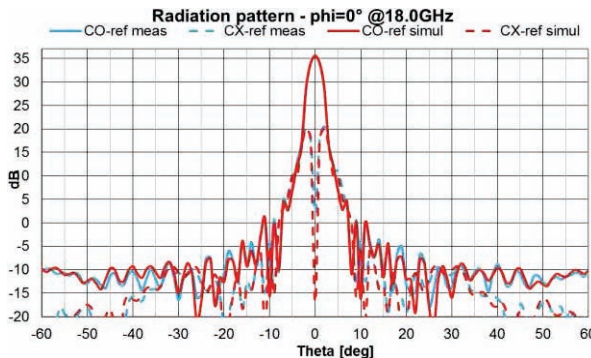


Figure 10. Measurement and simulation reference directivity patterns @18GHz, phi=0°.

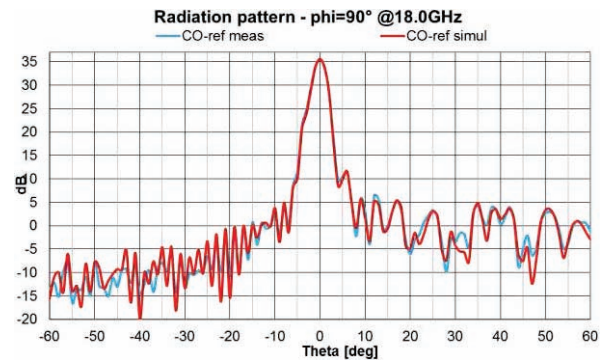


Figure 11. Measurement and simulation reference directivity patterns @18GHz, phi=90°.

C. Pattern Correlation/Equivalent Noise Level

The visible pattern agreement is confirmed by computing the pattern correlation or equivalent noise level:

$$EqNoise = 20 * \log \left[\text{StdDev} \left(\frac{Dir_{co, xp} - Dir_{ref_co, xp}}{Dir_{ref, boresight}} \right) \right] \quad (1)$$

where $Dir_{co, xp}$ is the directivity (or gain) of the copolar (or crosspolar) component, $Dir_{ref_co, xp}$ is the directivity (or gain) of the reference copolar (or crosspolar) component and $Dir_{ref, boresight}$ is the directivity (or Gain) of the reference copolar component at the boresight.

Correlation between measurement and simulation reference has been computed in a ±45° conical angle for both polarizations as reported in Table VI.

TABLE VI. EQUIVALENT NOISE LEVEL@10.7 AND 18 GHZ

Equivalent Noise Level [dB] @10.7 GHz		
Phi cut	CO	CX
0°	-49.37	-50.49
Equivalent Noise Level [dB]@18 GHz		
Phi cut	CO	CX
0°	-49.77	-50.23

D. Dissipation Loss Comparison

The measurement and simulation reference dissipation losses are reported in Table VII. Measured losses are obtained as the difference between the IEEE Gain and the Directivity, therefore the accuracy is related to the gain accuracy of the measurement facilities.

It seems that simulations underestimate the losses. A plausible explanation is connector losses, not included in the simulation scenarios and the uncertainty of the aluminum electrical conductivity considered in the simulations. The vendor sheet value has been used in the simulation with no experimental verification.

TABLE VII. DISSIPATION LOSS

Dissipation Loss [dB]		
Frequency	Measured	Simulated
10.7 GHz	-0.49	-0.09
18 GHz	-0.68	-0.17

E. Matching / Return Loss Comparison

The measurement and simulation reference return loss values are reported in Table VIII. At 18 GHz, in particular, some differences between simulations and measurements are visible. These can be explained from the differences in matching condition in the simulation scenario and the actual antenna. Simulations have been performed considering a discrete excitation port of the SH4000 with definitions depending on the numerical tool. Measurements are referred to a 50Ω high precision connector. For measurements, the return loss is available as a curve over the frequency band, which is more meaningful for the comparison and it is shown in Figure 12.

TABLE VIII. RETURN LOSS

Return Loss [dB]		
Frequency	Measured	Simulated
10.7 GHz	-12.89	-11.91
18 GHz	-16.84	-14.71

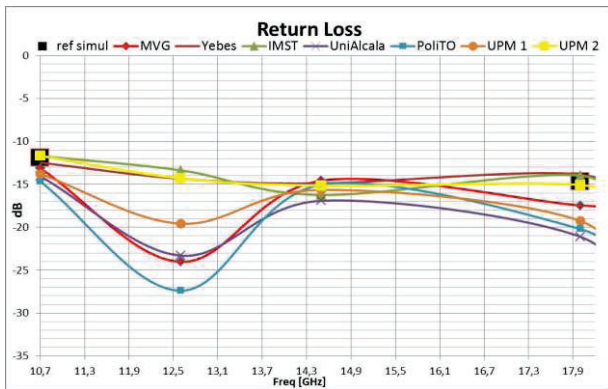


Figure 12. Return Loss as a curve over the frequency for measurements results (MVG, Yebes, IMST, UNIAIcalà, PoliTo, UMP1 and UPM 2) and 2 discrete points as reference for simulations.

VI. CONCLUSIONS

The achievable agreement between antenna measurement and numerical simulation has been investigated using many measurements and many simulations. The experiment has been designed to minimize error sources not pertinent to simulation/measurement. The agreement between simulation and measurements is deemed excellent, considering uncertainties due to simulation, measurement and manufacturing. The level of correlation between measurements and simulation achieved here are better than what has been found in recent facility comparisons campaigns. Very good agreement has been achieved for performance parameters such as peak directivity, pattern, and good agreement for gain contributions such as dissipation loss and matching.

REFERENCES

- [1] ANSI/IEEE Std 149-1979, "Standard Test Procedures for Antennas"
- [2] IEEE Std 1720 - 2012, "Recommended Practice for Near - Field Antenna Measurements"
- [3] www.cst.com, CST STUDIO SUITE™, CST AG, Germany
- [4] www.feko.info, Altair Engineering GmbH, Germany
- [5] www.ansys.com/Products/Simulation+Technology/Electronics/Signal+Integrity/ANSYS+HFSS, ANSYS Inc. USA
- [6] www.ticra.com, Denmark
- [7] http://www.empire.de
- [8] L.J.Foged, M.A. Saporetti, M. Sierra-Castanner, E. Jørgensen, T. Voigt, F. Calvano, D. Tallini, "Measurement and Simulation of Reflector Antenna", EuCAP2015, Lisbon, April 2015.
- [9] L. J. Foged, M. Sierra Castañer, L. Scialacqua "Facility Comparison Campaigns within EurAAP", 5th European conference on Antennas and propagation, EuCAP2011, Rome, April 2011.
- [10] A.C. Ludwig, "The Definition of CrossPolarization", IEEE Trans. Antennas Propagation, vol. AP-21 no.1, pp. 116-119, Jan. 1973.
- [11] X. Yuan, "Three-dimensional Electromagnetic Scattering from Inhomogeneous Objects by the Hybrid Moment and Finite Element Method," IEEE Transactions on Microwave Theory and Techniques, Vol. 38, No. 8, August 1990, pp. 1053-1058.
- [12] W. C. Chew, J. M. Jin, E. Michielssen, and J. M. Song, Fast and Efficient Algorithms in Computational Electromagnetics, Artech House, Boston, MA, 2001.
- [13] Poggio, A. J. and Miller, E. K., "Integral Equation Solutions of Three-Dimensional Scattering Problems." Computer Techniques for Electromagnetics, edited R. Mittra, Pergamon Press, New York, 1973
- [14] M. Sabbadini, G. Guida, M. Bandinelli, The Antenna Design Framework ElectroMagnetic Satellite, IEEE Antennas and Prop. magazine 05/2009
- [15] J. Jin, The Finite Element Method in Electromagnetics, Second Edition, John Wiley & Sons Inc., New York, NY, 2002.
- [16] O. Borries, P. Meincke, E. Jørgensen, and P. C. Hansen, "Multilevel Fast Multipole Method for Higher-Order Discretizations," IEEE Transactions on Antennas and Propagation, vol. 62, no. 9, pp. 4695-4705, Sep. 2014.
- [17] T. Weiland: "RF & Microwave Simulators - From Component to System Design" Proceedings of the European Microwave Week (EUMW 2003), München, Oktober 2003, Vol. 2, pp. 591 - 596.
- [18] B. Krietenstein, R. Schuhmann, P. Thoma, T. Weiland: "The Perfect Boundary Approximation Technique facing the big challenge of High Precision Field Computation" Proc. Of the XIX International Linear Accelerator Conference LINAC, Chicago, USA, 1998, pp. 860-862.
- [19] L.J. Foged, L. Scialacqua, F. Saccardi, F. Mioc, D. Tallini, E. Leroux, U. Becker, J. L. Araque Quijano, G. Vecchi: "Bringing Numerical Simulation and Antenna Measurements Together", EuCAP2014, The Hague, The Netherlands, April 2014